International Journal of Pharmaceutics 684 (2025) 126164

Contents lists available at ScienceDirect

International Journal of Pharmaceutics

journal homepage: www.elsevier.com/locate/ijpharm

Innovative bilayered buccal films: A paediatric-friendly dosage form for transmucosal azithromycin delivery

Giulia Bondi [a], Ilenia D'Abbrunzo [b], Dritan Hasa [b], Carola Parolin [a], Beatrice Vitali [a], Serena Bertoni [a], Anna Imbriano [c], Cinzia Pagano [c], Costanza Fratini [d], Beatrice Sabbatini [d], Federica Bigucci [a,1], Angela Abruzzo [a,1,*]

[a] University of Bologna, Department of Pharmacy and Biotechnology, Via San Donato 19/2, Bologna, Italy
[b] University of Trieste, Department of Chemical and Pharmaceutical Sciences, Piazzale Europa 1, Trieste, Italy
[c] University of Perugia, Department of Pharmaceutical Sciences, Via del Liceo 1, Perugia, Italy
[d] University of Urbino Carlo Bo, Department of Biomolecular Sciences, Via Ca le Suore 2, Urbino, (PU), Italy

ARTICLE INFO

Keywords:
Bilayered buccal films
Transmucosal administration
Children
Azithromycin
Permeation studies

ABSTRACT

Azithromycin (AZT) is one of the most prescribed antibiotics in children, generally administered through the oral route. However, its low aqueous solubility, poor oral bioavailability and bitter taste can affect the therapy efficacy and the children's compliance. In this study, different mucoadhesive polymers and solubilizers were explored to develop a primary layer capable of establishing a prolonged contact with the mucosa. An ethylcellulose layer was further applied to assure the drug unidirectional absorption through the buccal mucosa and limit its bitter taste in the mouth. Films were characterized for their thickness, drug content and solid state, morphology, hydration mucoadhesion and mechanical properties. *In vitro* drug release and permeation through the buccal mucosa as well as antimicrobial activity were also investigated. The selected compositions, based on chitosan (CS), alginate (ALG) or sodium hyaluronate (HYA) in association with Soluplus® or polyvinylpyrrolidones allowed to obtain uniform, thin and mucoadhesive films. CS films determined a quick AZT release, due to the presence of a new, more soluble form of the drug (confirmed by PXRD and FT-IR analysis) with unaltered antimicrobial properties. Conversely, HYA and ALG films showed a more sustained release. Interestingly, the presence of the backing layer, confirmed by morphological studies, hindered the drug release, thus demonstrating that films could limit AZT taste inside the mouth. Among all the formulations, HYA film was characterized by the best profile of drug permeation, allowing the retention of drug antimicrobial ability and can be proposed as a buccal delivery system for the systemic absorption of AZT.

1. Introduction

Antibiotics represent the most commonly used drugs in the paediatric population. Among all of them, azithromycin (AZT), a broad-spectrum macrolide, is generally indicated for the treatment of different infectious diseases, such as the upper and lower respiratory infections and the otitis media (Dung et al., 2023). Currently, AZT administration in children consists of the employment of oral formulations, like granules for suspension and extended-release microspheres (Swainston Harrison and Keam, 2007). Nevertheless, after oral administration AZT shows a low bioavailability (around 37 %), as consequence of its poor aqueous solubility (≈ 0.1 mg/mL), high degradation in the acidic pH of the stomach and incomplete absorption (Aucamp et al., 2015; Fiese and Steffen, 1990; Luke and Foulds, 1997; Tung et al., 2018). Moreover, it has been reported that AZT oral administration is responsible for side effects, such as nausea, vomiting and diarrhoea due to the local concentration of the drug in the gastrointestinal tract (Lo et al., 2009). Another important obstacle concerning AZT oral administration in children regards its extremely bitter taste (Mashaqbeh et al., 2024), highlighting the urgent need for the

* Corresponding author at: Department of Pharmacy and Biotechnology, University of Bologna, Via San Donato 19/2, 40127 Bologna, Italy.
E-mail addresses: giulia.bondi9@unibo.it (G. Bondi), ilenia.d'abbrunzo@phd.units.it (I. D'Abbrunzo), dhasa@units.it (D. Hasa), carola.parolin@unibo.it (C. Parolin), b.vitali@unibo.it (B. Vitali), serena.bertoni4@unibo.it (S. Bertoni), anna.imbriano@unipg.it (A. Imbriano), cinzia.pagano@unipg.it (C. Pagano), c.fratini2@campus.uniurb.it (C. Fratini), beatrice.sabbatini@uniurb.it (B. Sabbatini), federica.bigucci@unibo.it (F. Bigucci), angela.abruzzo2@unibo.it (A. Abruzzo).
[1] These authors contributed equally to the work.

https://doi.org/10.1016/j.ijpharm.2025.126164
Received 11 July 2025; Received in revised form 25 August 2025; Accepted 9 September 2025
Available online 10 September 2025

development of new taste-masked dosage forms for paediatric population.

Buccal route represents an interesting site for drug administration in children *in virtue* of several advantages like the direct absorption of the drug into the systemic circulation, thus bypassing the stomach, and the simple access for self-medication, improving both patient acceptance and compliance (Lam et al., 2014). In the field of buccal administration, mucoadhesive drug delivery systems represent a promising platform for drug delivery. As a matter of fact, the intimate contact between the mucoadhesive formulation and the buccal mucosa can determine a longer retention time of the drug at the application/absorption site, reducing at the same time the saliva wash-out effect which can determine the involuntary swallowing of formulation (Bagan et al., 2012). Among all the child-appropriate buccal dosage forms, films have been considered the most interesting formulations as they are thin, easily applicable and able to ensure accurate and flexible dosing (Lam et al., 2014). Furthermore, the application of a non-dissolvable backing layer on the mucoadhesive film allows to achieve the unidirectional drug release towards the buccal mucosa, avoiding it in the oral cavity and at the same time limiting the bitter taste perception in the mouth. Therefore, the aim of this study was to develop and characterize bilayered films for AZT buccal administration in children. The first goal was to select suitable mucoadhesive excipients useful to obtain a primary layer containing the drug. Specifically, different mucoadhesive polymers, such as hydroxypropylmethylcellulose, sodium hyaluronate, sodium alginate, xanthan gum, carrageenan and chitosan, were screened to obtain the primary layer through the solvent casting method. Moreover, particular attention was given to the identification of adequate strategies to include such a lipophilic drug, like AZT (log P = 4; Guimarães et al., 2021), in the mucoadhesive hydrophilic layer. In this context, several solubilizers, such as lecithin, casein, polyvinylpyrrolidone K25, polyvinylpyrrolidone K25 and Soluplus®, were selected. All these excipients are classified by the FDA as GRAS substances and applied in developing several paediatric formulations (Boza et al., 2025; Cornilă et al., 2022; Corzo-Martínez et al., 2015; Domingues et al., 2023). To the best of our knowledge, this is the first study investigating the association of so many different polymers and solubilizers to achieve the delivery of a lipophilic drug. Moreover, to date, no works have been published concerning the development of buccal films intended for systemic AZT administration. A single study reported the use of a buccal patch containing AZT (Latif et al., 2016) for the local release of the drug. The patch was composed solely of HPMC, and no information was provided regarding drug content, mucoadhesive properties, *in vitro* drug release or permeation. The authors proposed the patch for the treatment of chronic periodontitis in adults and evaluated different parameters linked to this disease condition. In another study, ocular films of AZT were prepared using alginate, carbopol, and hydroxypropyl methylcellulose by the film casting method and subsequently subjected to characterization (Gilhotra et al., 2011).

The second goal of the present study regards the achievement of the unidirectional drug absorption and of AZT bitter taste masking. For this purpose, a backing layer based on ethylcellulose was applied to the primary mucoadhesive layer to limit the drug release in the buccal cavity. In our previous work, we had developed bilayered films for systemic delivery of propranolol hydrochloride, an active hydrophilic molecule with a well-known bitter taste (Abruzzo et al., 2017). Ethylcellulose had been solubilized in acetone and sprayed on the primary polymeric layer. The challenge of the present study was to avoid the repartition of AZT from the primary mucoadhesive layer to the backing layer, through drug solubilization in acetone during the spraying and drying, Films were deeply characterised in terms of thickness, drug content, drug solid state, morphology, water uptake ability, mucoadhesion, mechanical properties, *in vitro* drug release and permeation, and antimicrobial activity. Another innovative aspect of our study regarded the discovery of a new form of the drug, which presents interesting properties in terms of improved solubility, opening new perspectives able to overcome the most important drawbacks of AZT.

2. Materials and methods

2.1. Materials

Hydroxypropylmethylcellulose (HPMC; Benecel™ K100M PHARM, MW 1000 kDa) was sourced from Ashland (Ashland, Switzerland). Sodium alginate (ALG; MW140 kDa) and sodium hyaluronate (HYA; MW 1800–2300 kDa) were purchased from Farmalabor (Canosa di Puglia, Italy). Xanthan gum (XG; MW 10,000 kDa) was supplied from ACEF (Piacenza, Italy). Polyvinylpyrrolidone K25 (PVP K25; MW 24 kDa) and polyvinylpyrrolidone K90 (PVP K90; MW 70–90 kDa) were obtained from Fluka (Milan, Italy). Ethylcellulose (ETHOCEL1 Standard E10 FP Premium, viscosity range 9–11 mPa x s) and Soluplus® (SOL, 90–140 kDa) were a kind gift from Colorcon Ltd (Dartford, England) and BASF SE (Ludwigshafen, Germany), respectively. Carragenaan (CAR; MW 193–324 kDa), low-viscosity chitosan (CS; MW 150 kDa, deacetylation degree 97 %; pKa = 6.3), lecithin (LEC), casein (CAS), azithromycin dihydrate (AZT) and all the other chemicals were purchased from Merck (Milan, Italy).

Water-uptake, residence time, and release studies were carried out in aqueous buffer having the following composition (g/L): 4.61 KH_2PO_4 and 16.75 Na_2HPO_4 x12H_2O adjusted to pH 6.8 with H_3PO_4 1 % v/v (healthy saliva pH = 6.7–7.4)(Gittings et al., 2015; Marques et al., 2011). Permeation studies were performed in buffer solution at pH 7.4 (g/L): 2.38 Na_2HPO_4 x12 H_2O, 0.19 KH_2PO_4 and 8.0 NaCl.

2.2. Preparation of bilayer films

Different mucoadhesive polymers were screened for the preparation of the primary layer. Specifically, HPMC, ALG, HYA, XG or CAR were solubilized in water (2 % w/v), while CS was dissolved (2 % w/v) in lactic acid (1.6 % v/v). All solutions were left under stirring at 300 rpm for 24 h. Furthermore, different solubilizers were employed in order to facilitate AZT incorporation inside the primary layer. Particularly, LEC (2 % w/v), CAS (2 % w/v) and SOL (2.5 % w/v) were dissolved in water under stirring at 300 rpm for 72 h, instead PVP K25 and PVP K90 (2 % w/v) for 24 h. Polymeric- and solubiliser-based solutions were then mixed (1:1, w/w) and stirred for 45 min before adding glycerol (1 % w/w for HPMC, ALG, HYA, XG, CAR and 0.5 % w/w for CS), employed as plasticizer. Loaded films were prepared by dispersing AZT (30 mg/mL) in the solubilizer solution, before the mixing. The mixtures were subsequently placed in a silicon mould (13 g in a diameter of 5 cm) and oven-dried (heating oven FD series, Binder, Tuttlingen, Germany) at 70 °C for 7 h. For bilayered film preparation, a previously published method was followed, with slight modifications (Abruzzo et al., 2017). Briefly, an ethylcellulose solution (5 mL, 1 % w/w in acetone) was sprayed on the primary polymeric layer (1 cm^2) in small portions (0.3 mL), with each application immediately followed by oven-drying at 70 °C for 5 min (this process was repeated until the entire 5 mL were applied). After preparation, films were stored in a well-closed container at room temperature. Films were evaluated for their physical characteristics i.e., colour (visual inspection), transparency (against white light), peelability (removal of film after drying) and homogeneity (visually against white light).

2.3. Solution viscosity

The viscosity of the solutions employed for the preparation of the primary polymeric layer was measured using a falling ball viscometer at room temperature (24 – 26 °C) (HAAKETM Falling Ball Viscometer Type C. Thermo electron corporation, Karlsruhe, Germany).

2.4. Film weight, thickness and pH

Films having a surface area of 1 cm^2 from different batches as well as different portions of the same film (obtained from one mould) were cut and the mean weight of five randomly selected samples from each formulation was measured using an electronic balance (Sartorius, Milan, Italy). Film thickness was measured using an electronic digital caliber (art. 1367 E 2900, Shanghai ShangErBo Import & Export Co., Shanghai, China). For the pH measurement, films with a surface area of 1 cm^2 were kept in contact with 5 mL of phosphate buffer solution at pH 6.8; then the solutions were filtered, and the pH was determined with a digital pH meter (pH meter, MicroPH CRISON 2000, Modena, Italy). To exclude the influence of the buffer, films (1 cm^2) were placed in 5 ml of distilled water for 30 min. After this time, the swollen films were taken out, drained, and the pH value of the film surface was measured with an indicator strip pH 6 – 7.7 (Macherey-Nagel, Düren, Germany)(Al-Dhubiab et al., 2016; Muzib and Kumari, 2011).

2.5. Drug content

To determine the drug content, three film units with a surface area of 1 cm^2 taken from different batches as well as different portions of the same film were placed in 5 mL methanol for 24 h under magnetic stirring (300 rpm). Then 100 μL of the solution were withdrawn, diluted in methanol and analysed using a HPLC method (section 2.6) in order to determine the amount of AZT in each film.

2.6. HPLC conditions

AZT quantification through HPLC was performed following the method previously reported (Abruzzo et al., 2022). The chromatographic system was composed of a Shimadzu (Milan, Italy) LC-40D chromatographic pump and a Shimadzu SPD-10AVP UV–vis detector set at 215 nm. Separation was obtained on a Phenomenex (Torrance, CA, USA) Kinetex (150 mm × 4.6 mm I.D., 5 mm) coupled to a Phenomenex (Torrance, CA, USA) Security Guard C18 guard cartridge (4 mm × 3.0 mm I.D., 5 mm). The mobile phase was prepared by mixing a buffer (KH_2PO_4 0.01 M adjusted at pH 7.5 with KOH 0.1 M) with methanol and acetonitrile (10/50/40, v/v/v). The flow rate was 0.8 mL/min and manual injections were made using a Rheodyne 7125 injector with a 20 μL sample loop. Data processing was handled by means of a CromatoPlus computerized integration system (Shimadzu Italia, Milan, Italy). Calibration curve of concentration versus peak area ratio was plotted at concentration range of 10 – 500 μg/mL and a good linearity was found ($R^2 = 0.9996$). The method was further validated with respect to characteristics like specificity in the presence of excipients, precision, Limit of detection (LOD), Limit of quantification (LOQ) and stability ("Guideline on Validation of Analytical Procedures," 2022). Specificity was demonstrated, showing that neither formulation excipient interfered with the quantification of AZT. The method's precision (determined by injecting the working standard six times in succession) yielded a relative standard deviation (RSD) below 2.5 %. LOD and LOQ were found to be 2.5 μg/mL and 7.5 μg/mL, respectively. As regards the stability (determined by using the same working standard for 0, 1, 2, 4, 6 and 8 h), RSD values were below 2 %.

2.7. Differential scanning Calorimetry (DSC)

DSC analysis was performed in order to evaluate the drug solid state in films. A Perkin Elmer DSC 6 (Perkin Elmer, Beaconsfield, UK) with nitrogen as a purge gas (20 mL/min) was employed. Films, weighing about 2–3 mg, were placed in an aluminum pan and heated from 30 to 200 °C at a scanning rate of 10 °C/min.

2.8. Powder X-ray diffraction (PXRD) analysis

PXRD analyses were carried out using a Bruker D2 Phaser benchtop diffractometer (Bruker, Manheim, Germany), using Cu-Ka radiation (λ = 1.5418 Å) with a 300 W low-power X-ray generator (30 kV at 10 mA). All the measurements were conducted in a 2q range of 5-35° with a step size of 0.02° and a scan speed of 0.6°/s. Every sample was placed on a "zero background" sample holder coated with silicone resin.

Both drug-free and drug-loaded buccal films were characterised through PXRD to confirm the presence of the drug and assess its physical form (e.g., crystalline AZT as the starting material, amorphous state, polymorphic form, etc.).

2.9. Scanning electron microscopy (SEM)

Images of AZT-loaded buccal films were collected through SEM. The samples were placed on aluminum stubs covered with a carbon double-sided before being analysed by a scanning electron microscope (Quanta 250 SEM, FEI, Oregon, USA) with the secondary electron detector. The working distance was set at 10 mm to obtain the appropriate magnifications, and the acceleration voltage was set at 30 kV. Cross-sectional images were acquired for the bilayer films to clearly identify and distinguish the coating layer from the underlying film matrix.

2.10. Fourier-transform Infrared spectroscopy attenuated total Reflectance (FT-IR ATR)

To investigate the potential interaction between AZT and lactic acid, AZT (15 mg/mL) was first dissolved in a 0.8 % v/v aqueous solution of lactic acid under continuous magnetic stirring (300 rpm) for 24 h. The resulting solution was oven-dried at 70 °C for 7 h, yielding a pasty-like solid residue (referred to as AZT-lac). This product was then analysed using FT-IR ATR spectroscopy to assess possible molecular interactions. Spectra were acquired for AZT-lac, pure AZT, and pure lactic acid using a Shimadzu IRAffinity-1S spectrometer (Kyoto, Japan) equipped with an ATR accessory, within the 400–4000 cm^{-1} range, at a resolution of 4 cm^{-1} and with 20 accumulated scans.

2.11. Water uptake ability

Water uptake studies were carried out to measure the hydration ability of primary polymeric layers and bilayered films by following a previous method (Abruzzo et al., 2017). An accurately weighted square of film with a surface area of 0.49 cm^2 (0.7 cm x 0.7 cm) was placed on filter paper (4 cm x 4 cm) soaked in phosphate buffer at pH 6.8 and positioned on the top of a sponge (11 cm x 6.5 cm x 2 cm), previously soaked in the hydration medium. The sponge was placed in a Petri dish (diameter 22 cm) filled with the same solution to a height of 0.5 cm. At specified time intervals the film and the wet paper filter were weighted and subsequently repositioned on the sponge.

Water uptake (WU) was determined as weight increase of the film for 360 min, according to the following equation:

$$WU(\%) = \frac{(WH_{fp} - WH_p - WD_f)*100}{WD_f}$$

where WH_{fp} is the weight of hydrated film and wet paper filter, WH_p is the weight of wet paper filter and WD_f is the weight of the dry film.

2.12. In vitro mucoadhesion ability and residence time

Mucoadhesion ability was determined by measuring the force necessary to pull out a freshly oesophageal mucosa from primary polymeric layers. In previous studies, it was demonstrated that porcine esophageal mucosa is comparable to the buccal one and it has been selected as the preferred model (Diaz del Consuelo et al., 2005). Pig

esophageal tissue was obtained from a local abattoir (CLAI, Faenza, Italy). Mucosa was separated from the muscular layer by cutting the connective fibers with a scalpel. For this measurement an adapted tensiometer (Krüss 132869; Hamburg, Germany) was used (Abruzzo et al., 2017). The esophageal mucosa was attached with cyanoacrylate adhesive to a support (surface area 1 mm^2) and hydrated with 50 μL of mucin solution (0.05 % w/v in phosphate buffer at pH 6.8) for 2 min. Then the mucosa was lowered on a piece of film (1 cm^2) fixed to a microscope glass with cyanoacrylate adhesive and a force of 20 dyne was applied for 1 min. Subsequently, the mucosa was raised up until it fully separated from the film.

Residence time measurements were performed to evaluate the time needed for the complete detachment of films from the mucosa in phosphate buffer at pH 6.8 (Abruzzo et al., 2017). For this study the mucosa (surface area 4 cm^2) was attached to a glass slide using cyanoacrylate adhesive and then hydrated with 20 μL of mucin 0.05 % (w/v) in phosphate buffer at pH 6.8. After 2 min a piece of film (1 cm^2) was attached to the mucosa with a slight pressure and allowed to adhere for 15 min. Subsequently, the glass slide was immersed in a beaker containing 20 mL of the buffer. The time required for the film detachment from the mucosa was recorded using a digital chronometer. This test was carried out on both bilayer film and primary layer.

2.13. In vitro release studies

In vitro release studies were performed to determine the amount of drug released over time from primary layers and bilayered films. To execute this test, a piece of primary layer (1 cm^2) was fixed to a glass slide with cyanoacrylate adhesive and left to adhere for 30 min. For the evaluation of drug release from bilayered films, the films were attached on the glass side with the ethylcellulose layer facing towards the medium. They were then immersed in a beaker with 20 mL of phosphate buffer at pH 6.8. After 30, 60, 120, 180, 240, 300, and 360 min, 500 μL aliquots were withdrawn and replaced with fresh medium. A control composed of AZT (Ctrl), as well as the AZT-lac prepared as described in section 2.9 (same amount as in the films) was tested. The samples were diluted and analysed using the HPLC method previously described. Results are shown as a percentage of Mt/M0, where Mt represents the amount of AZT released at each time and M0 the total AZT mass contained in the film, plotted as a function of time.

2.14. Mechanical properties

The burst strength (N) of the AZT-loaded films was explored using a texture analyzer (TA.XT plus Texture Analyzer, Stable Micro Systems, UK). A customized 3D printed apparatus presenting a 1 cm gap was realized via 3D printing as support for attaching the samples and was mounted on the working stage of the texture analyzer. For all measurements, the system was set in compression mode and equipped with a 50 Kg loading cell and P/2 mm cylinder probe. A 100 % strain was selected to record the force needed to completely break the film. Trigger force and test speed were set at 0.05 N and 1 mm/s, respectively. Considering the maximum peak of the force-distance plot, the burst strength needed to break the films was recorded. Also, the maximum applied pressure was calculated and expressed in MPa. For each formulation, at least a triplicate measurement was carried out and results were expressed as mean ± standard deviation.

2.15. In vitro permeation studies

In vitro permeation studies were conducted to quantitatively assess the ability of the drug to diffuse from primary monolayer or bilayered films across the buccal mucosa or to be retained inside it.

Franz-type static glass diffusion cells (15 mm jacketed cell with a flat ground joint and clear glass with a 12 mL receptor volume; diffusion surface area = 1.77 cm^2), equipped with a V6A Stirrer (PermeGearInc., Hellertown, PA, USA) were employed. Porcine oesophageal epithelium was used to separate the donor and receptor compartments. To isolate the epithelium, the excised oesophageal mucosa was immersed in saline solution (NaCl 0.9 % w/v) at 60/65 °C for 1 min. After the epithelium was peeled from the connective tissue and placed over a 0.45 μm cellulose acetate filter with the connective side in contact with the filter. The epithelium was placed between the donor and the receiving chamber of the Franz cells and hydrated with 200 μL of phosphate buffer at pH 6.8. Films (1 cm^2) or the drug powder in the same amount contained in the films (Ctrl) were located in the donor chamber. The receptor compartment was composed of 12 mL of a mixture of phosphate buffer solution at pH 7.4 and ethanol in a proportion 80:20 v/v, maintained at 37 °C by means of a surrounding jacket and constantly stirred to assure a uniform drug concentration. At predetermined time intervals (30, 60, 120, 180, 240, 300 and 360 min), 200 μL samples were collected from the receptor compartment, replaced with the same amount of fresh medium and analysed using HPLC. The results of permeation studies are shown as a percentage of the cumulative permeated drug plotted as a function of time. Cumulative amounts of drug permeated per unit area of the epithelium (μg/cm^2) was also plotted against time (min). Flux (J) was generated from the slope of the linear portion of the curve.

After 360 min, the residual formulations contained in the donor compartment were removed and the epithelium was carefully washed with methanol (0.5 mL). Then, the epithelium was dismounted from the apparatus and placed in methanol (5 mL) for 5 h under magnetic stirrer (300 rpm) to extract the drug. The epithelium was subsequently withdrawn and the solution was centrifuged at 14,500 rpm for 20 min (GS-15R Centrifuge, Beckman Coulter, Milan, Italy) and analysed through HPLC to determine AZT amount retained within the tissue.

2.16. Antimicrobial properties

Antimicrobial properties of films were evaluated against *Staphylococcus aureus* ATCC 29213 and *Escherichia coli* ATCC 11105, chosen as representative Gram-positive and Gram-negative bacteria, respectively. Bacterial strains were routinely grown in Brain Heart Infusion medium (BHI, Difco, Detroit, MI), at 37 °C. Bacterial suspensions were prepared at a concentration of $2x10^6$ CFU (colony forming units)/mL in 2x BHI broth. Minimal Inhibitory Concentrations (MIC) of AZT were determined by a microdilution assay carried out on a 96-well plate, following NCCLS standard guidelines (Cockerill, 2012; Lugli et al., 2025). Loaded films (1 cm^2) were placed in a beaker with 20 mL of phosphate buffer at pH 6.8. After 360 min solutions containing the released drug were withdrawn and diluted with the same buffer to obtain a final drug concentration of 60 μg/mL. A control was prepared by dissolving the drug in the buffer at the same concentration. Subsequently, the samples were 2-fold serially diluted in the buffer and added to the bacterial suspensions in equal amounts, in order to reach AZT concentrations in the range 0.05–30 μg/mL. Unloaded films were also tested following the same procedure and applying the same dilutions. MIC values were determined after 24 h of incubation at 37 °C.

2.17. Statistical analysis

All results are shown as mean ± standard deviation (SD). SD was calculated from the values of three independent experiments, except for the permeation results, which were calculated from the values of at least five independent experiments. Data from all experiments were analysed using a *t*-test, and differences were deemed significant for $p < 0.05$.

3. Results and discussion

3.1. Preparation of bilayer films

The preparation process of the final formulations was based on different steps. First, a screening was conducted to select the polymers

able to provide films. In this context, various mucoadhesive polymers, hydroxypropylmethylcellulose (HPMC), chitosan (CS), sodium alginate (ALG), sodium hyaluronate (HYA), xanthan gum (XG) and carrageenan (CAR), were tested with the aim of developing a final formulation capable of prolonged retention within the buccal cavity. In a preliminary evaluation, solutions without drug and solubilizers were prepared by dissolving the investigated polymers in water, except for CS whose solubilization required an acidic environment. In this latter case, lactic acid was preferred over the most employed acetic acid. In fact, it has been reported that films containing acetic acid were characterised by a strong, potent odour of vinegar, which can be difficult to accept, especially by children (Korelc et al., 2023). The solvent casting method was selected for film preparation due to its simplicity and cost-effectiveness. Indeed, all the prepared polymeric solutions, with the exception of the not uniform CAR-based one, were cast. The obtained films were homogeneous and easy to handle and to remove from the mould without damage, excluding XG film which presented cracks. For this reason, the latter was excluded from the further steps.

Secondly, to favour AZT ((lipophilic molecule, logP = 4; (Guimarães et al., 2021)) inclusion within the polymeric solutions, different solubilizers, such as casein (CAS), lecithin (LEC), Soluplus ® (SOL), and polyvinylpyrrolidones (PVPs) were tested. Preliminarily, unloaded films were prepared to explore if the different compositions were able to provide films. All the selected polymers (HPMC, CS, ALG and HYA) were combined with CAS, LEC, SOL, PVPs. All the combinations provided uniform and easily handled films. CAS and LEC produced films with an unpleasant odour, which could negatively impact patient acceptability − particularly in the paediatric population − and were therefore excluded from further development. Moreover, the association of the polymers with PVPs allowed to obtain transparent films, while in the presence of SOL opalescent films were produced. This result was due to the presence of SOL micelles in the polymeric solutions which were characterised by a slight opalescence. In order to verify the presence of micelles in our preparations, a solution of SOL (12.5 mg/mL) was adequately diluted in water (18.2 MW cm, MilliQ apparatus by Millipore, Milford, MA, USA) and analysed through a Brookhaven 90-PLUS instrument (PCS, Brookhaven Instruments Corp., Holtsville, NY, USA) with an He-Ne laser beam at a wavelength of 532 nm (scattering angle of 90°). The analysis confirmed the presence of micelles whose sizes were equal to 57 ± 4 nm. From these findings, it was possible to conclude that HPMC, CS, ALG and HYA can be associated with the solubilizers SOL and PVPs. Overall, this preliminary screening offers valuable insights for the development of buccal films able to deliver hydrophilic and lipophilic drugs and could be exploited in the future to deliver other active compounds.

Subsequently, the impact of AZT inclusion on physical characteristics of the primary layer was evaluated and reported in Table 1.

As can be seen from Table 1, loaded films based on HPMC/SOL, HPMC/PVPs, ALG/PVPs and HYA/PVPs, were characterised by a non-uniform aspect and for this reason were discharged from the study.

Table 1
Loaded film characteristics.

Polymer	Solubilizer		
	SOL	PVP K25	PVP K90
HPMC	Not homogenous film	Not homogenous film	Not homogenous film
CS	Peelable, slightly opalescent and homogenous film	Peelable, transparent and homogenous film	Peelable, transparent and homogenous film
ALG	Peelable, slightly white and homogenous film	Not homogenous film	Not homogenous film
HYA	Peelable, slightly white and homogenous film	Not homogenous film	Not homogenous film

Instead, films composed of CS/SOL, CS/PVPs, ALG/SOL and HYA/SOL were uniform, easily handled and peelable from the mould, even if different characteristics were observed. In fact, CS/PVPs films were transparent, CS/SOL was slightly opalescent, while ALG/SOL and HYA/SOL films were opalescent. This behaviour was attributed to the solubility of the drug in the starting polymeric solutions. Specifically, the CS-based solutions containing lactic acid exhibited an acidic pH (~4.5), which enabled the solubilization of AZT (pKa ~ 8.5) by promoting the protonation of its amino groups, resulting in clear, transparent solutions. To evaluate drug solubility in lactic acid solution (1.6 % w/v adjusted at pH 4.5 with NaOH 5 % w/v), an excess of AZT was placed in 2 mL of the medium under magnetic stirring (300 rpm) for 72 h at room temperature. After this period, the samples were centrifuged at 8770 g for 30 min, filtered using a 0.22 μm acetate cellulose syringe filter and diluted before HPLC analysis. The obtained results confirmed our hypothesis and showed that the acidic pH particularly increased drug solubility (5.27 ± 0.27 mg/mL) with respect to the solubility in water previously determined (0.14 ± 0.02 mg/mL) (Abruzzo et al., 2022). However, the acidic environment alone was not sufficient to produce homogeneous films. In fact, when a drug-loaded solution based solely on CS was prepared and cast, the resulting film appeared non-homogeneous, confirming the necessity of incorporating an additional solubilizing agent. Indeed, SOL or PVPs were employed to improve the final properties of CS films. Drug solubility was also calculated in the presence of SOL or PVP at the same concentration as those used in the final film forming solutions (10 mg/mL for PVPs and 12.5 mg/mL for SOL), by following the procedure mentioned above. Drug solubility in the presence of SOL and PVP was equal to 0.43 ± 0.06 mg/mL and 0.28 ± 0.03 mg/mL, respectively (no significant difference was observed between PVP K25 and PVP K90; $p > 0.05$). The latter results were related to the ability of PVP and SOL to increase the solubility of lipophilic drugs. Particularly, it is well known that hydrophobic segments of PVP can form complexes with hydrophobic drugs, influencing their solubility, dissolution, and stability (Kurakula and Rao, 2020; Teodorescu and Bercea, 2015). SOL promotes drug solubilization thanks to its ability to spontaneously form micelles at concentrations higher than its critical micellar concentration (CMC = 7.6 mg/L; (Jiang et al., 2019)). To investigate the presence of loaded micelles, solutions of SOL (12.5 mg/mL) and AZT (15 mg/mL) were prepared and left under stirring for 72 h at 300 rpm. After that, the suspension was centrifuged at 8770 g for 30 min to remove the excess of drug in suspension, and the supernatant was dispersed in ultrapure water with a dilution of 1:1000 (v/v). Micelle formation was verified through PCS. The isolated supernatant contained micelles of 73 ± 10 nm, which were greater ($p > 0.05$) than the unloaded ones, probably due to the incorporation of AZT within the micelles. The presence of loaded micelles determined the slight opalescence in CS/SOL film. Finally, the selection of the drying temperature (70 °C) was done with the final aim of avoiding the thermal degradation of the drug. In this regard, a previous study reported (Timoumi et al., 2014) that in the solid state, AZT dihydrate undergoes only dehydration up to ~ 80 °C, without evidence of chemical degradation or lattice disruption.

To sum up, the presence of PVPs or SOL, in association with the acidic pH of the CS-based solution, allowed us to obtain transparent or slightly opalescent, easily handled and peelable films with a final homogenous aspect. Therefore, it can be assumed that in CS/PVP and CS/SOL, AZT was predominantly dissolved (*in virtue* of the presence of lactic acid and PVPs) and/or dispersed in micelles (only in the case of CS/SOL based film). Conversely, ALG and HYA with PVPs or SOL led to the formation of white solutions containing a high amount of drug in suspension in addition to the dissolved drug amount (as free molecules or in micelles in the presence of SOL). Anyway, for both ALG and HYA the addition of PVPs was not sufficient to assure the formation of homogeneous films, while in the presence of SOL (for both ALG and HYA) homogenous, milky-coloured and peelable final films were obtained.

Films having the selected compositions were coated with the ethylcellulose backing layer and named as follows: CS/PVP K25, CS/PVP

K90, CS/SOL, ALG/SOL and HYA/SOL.

3.2. Solution viscosity

The viscosity of the starting polymeric solutions can significantly affect the ability of the resulting films to promote drug release. In general, high-viscosity polymeric solutions tend to form viscous gels upon hydration, which may hinder drug diffusion (Abruzzo et al., 2017).

Based on this consideration, the viscosity of the initial solutions was measured. As shown in Table 2, ALG and HYA solutions exhibited significantly higher viscosity values compared to CS ($p < 0.05$), likely due to differences in molecular weight. Higher molecular weight polymers typically produce more viscous solutions. Additionally, the presence of PVPs led to an increase in viscosity compared to SOL ($p < 0.05$).

3.3. Film weight, thickness and pH

Film weight, thickness and pH were evaluated by using different batches as well as different portions of the same film (obtained from one mould). As can be observed in Table 2, film weight ranges between 28.8 to 33.6 mg/cm^2 and 39.7 to 46.1 mg/cm^2 for the primary layers and bilayer films, respectively and no significant differences were observed between all the formulations ($p > 0.05$). In all cases, an increase in film weight was observed for the bilayered films with respect to the primary layer ($p < 0.05$), thus demonstrating the successful backing procedure. Furthermore, the low standard deviation suggested that the method employed for film formation allowed to obtain uniform samples. The weight uniformity is a crucial issue considering that it directly influences the distribution of the drug inside the formulation and consequently the accuracy of the dosage.

Another important consideration for film designed for buccal administration is the thickness. As a matter of fact, it has been reported that the ideal thickness for a buccal film intended for the paediatric population is between 0.050 mm and 1 mm (Nair et al., 2013). Films with thickness value inside this range can maintain a strong and prolonged contact with the buccal mucosa, avoiding at the same time any discomfort upon application and consequently increasing patient acceptance and compliance. Moreover, the homogeneity in thickness value is strictly linked to the drug content uniformity. As can be seen from Table 2, the film thickness was within the range previously reported and varied from 0.18 to 0.24 mm and from 0.33 to 0.39 mm for the primary layers and bilayer films, respectively. Also, in this case a low standard deviation was registered, demonstrating the uniformity of the samples. Furthermore, the increase in thickness for bilayered films with respect to the primary layer ($p < 0.05$) represented a further proof of the success of the backing process.

Finally, the film pH was measured to evaluate the safety of the formulation and exclude a potential irritation of the buccal mucosa. The pH of the prepared films, both measured in phosphate buffer and in water, ranged between 6.5 and 7.0, aligning well with the physiological pH of the buccal cavity (typically 5.5–7.0) (Abdella et al., 2022). These values suggest that the films are suitable for buccal administration, minimising the risk of mucosal irritation.

3.4. Drug content

The determination of AZT content is crucial to verify its uniformity. Films (1 cm^2) from different batches and portions were used for AZT content determination (Table 2). The drug content/g of film was found to be 0.22 ± 0.01 g/g and no significant difference was observed between all the samples ($p > 0.05$). Moreover, the experimental drug content/cm^2 was very close to the theoretical one (9.94 mg/cm^2) for each formulation. The low standard deviations confirmed that the drug was uniformly distributed.

3.5. DSC

DSC analyses were carried out to investigate the physical state of the drug within the film. Generally, a shift in the drug's endothermic peak may suggest the occurrence of molecular interactions, whereas the complete disappearance of the peak typically indicates a transformation of the solid state. (Giordani et al., 2020; Timur et al., 2019). As can be seen from Fig. 1, the DSC profile of AZT showed a single endothermic peak at 120 °C, due to its melting, in agreement with previous findings (Kauss et al., 2013). The film profiles did not present remarkable endothermic events related to the drug, except for CS-based films, which showed an endothermic peak close to the melting point of the drug. These data indicated that in ALG- and HYA-based films the drug presented a low degree of crystallinity or an amorphous state. On the other hand, in the case of CS-based films, the slight shift of the drug endothermic peak could be related to a possible interaction of AZT with excipients used for film preparation. In order to better investigate the drug's solid state and any interaction between the drug and the other components of the films, powder X-ray diffraction analyses were performed.

3.6. Powder X-ray diffraction (PXRD) analyses

PXRD analyses were conducted on both unloaded and loaded buccal films and compared with the diffractogram of pure AZT. As expected, unloaded films exhibited amorphous profiles. Among the drug-loaded films, only those formulated with ALG/SOL and HYA/SOL (reported in Fig. 2) showed diffraction peaks attributable to crystalline AZT (see light orange lines in Fig. 2), although slight shifts of the characteristic peaks of AZT were observed in both cases, possibly due to interactions between the drug and the polymer matrix during film formation.

The remaining three films include CS as part of the polymeric matrix, in combination with a second polymer. Unlike the HYA/SOL and ALG/SOL films, where the presence of crystalline drug was confirmed by PXRD, the presence of AZT was no longer detectable in its original crystalline form in these CS-based systems. Instead, all three CS-containing films exhibited distinct diffraction patterns that did not match those of pure AZT or any of the individual formulation components. Interestingly, this new PXRD pattern was identical across all three formulations, regardless of the second polymer used (red patterns in Fig. 3), possibly suggesting the formation of a new solid phase.

Table 2
Viscosity of the starting polymeric solutions and film properties (weight, thickness and drug content expressed as AZT amount/g of film and AZT amount/cm^2).

Film	Viscosity of solutions (mPa x s)	Weight (mg/cm^2)		Thickness (mm)		Drug content (g/g)	Drug amount (mg)/cm^2
		Primary layer	Bilayered films	Primary layer	Bilayered films		
CS/PVP K25	69.78 ± 0.76	32.6 ± 1.3	45.1 ± 1.9	0.18 ± 0.02	0.38 ± 0.06	0.22 ± 0.02	9.81 ± 0.83
CS/PVP K90	80.42 ± 0.57	32.0 ± 3.1	46.4 ± 4.5	0.24 ± 0.05	0.33 ± 0.08	0.21 ± 0.02	9.83 ± 0.86
CS/SOL	57.33 ± 0.76	33.6 ± 3.3	46.1 ± 4.5	0.19 ± 0.06	0.36 ± 0.13	0.23 ± 0.01	9.90 ± 0.15
ALG/SOL	101.27 ± 0.45	29.5 ± 1.3	39.7 ± 1.8	0.22 ± 0.05	0.39 ± 0.05	0.24 ± 0.02	9.75 ± 0.32
HYA/SOL	151.03 ± 0.45	28.8 ± 1.9	42.1 ± 2.7	0.23 ± 0.06	0.36 ± 0.04	0.23 ± 0.03	9.70 ± 0.11

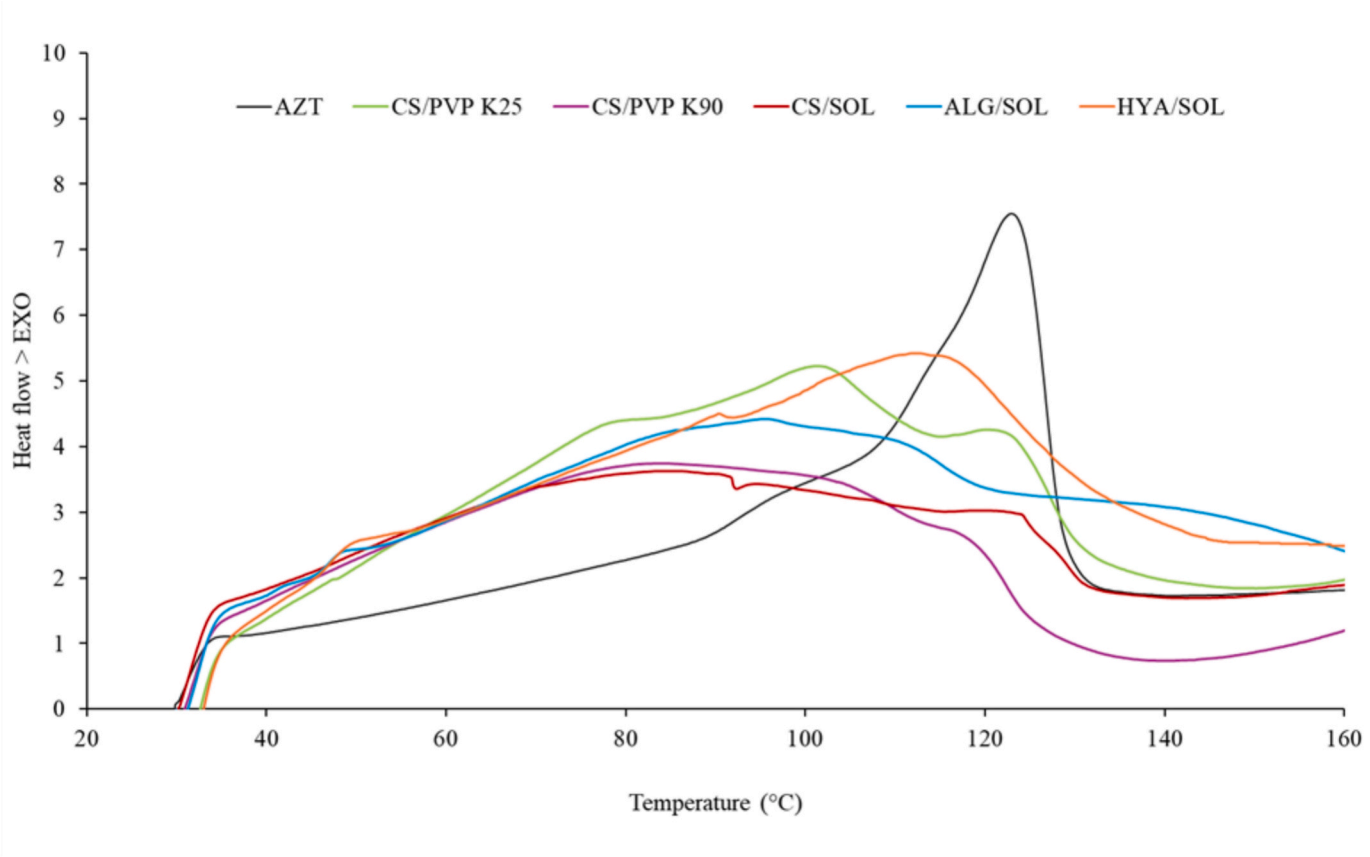

Fig. 1. DSC thermograms (30–160 °C) of AZT and loaded primary polymeric layers.

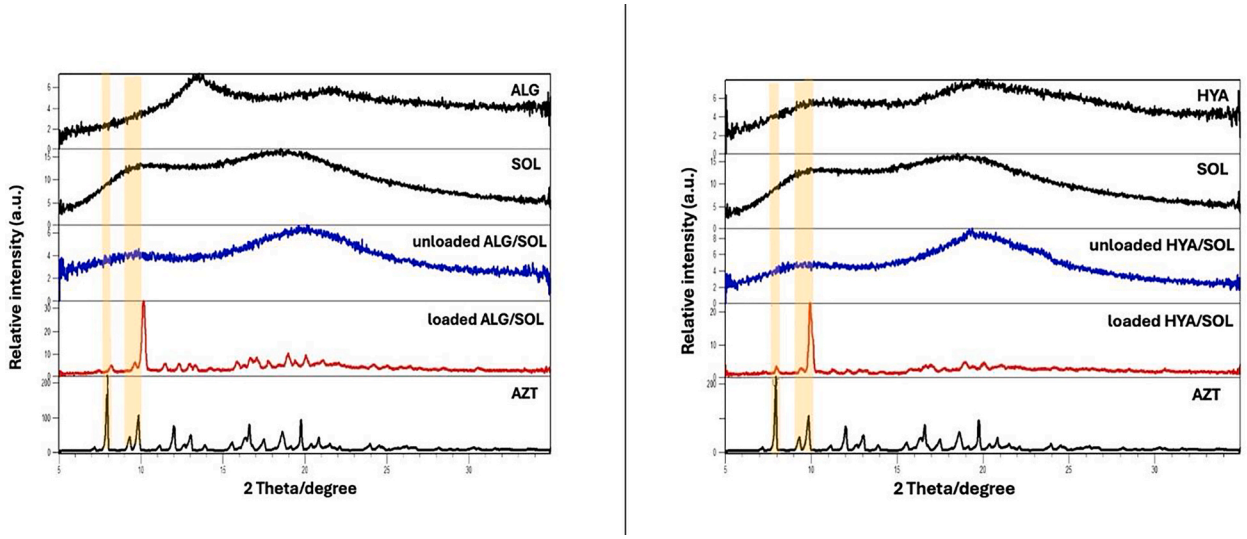

Fig. 2. PXRD of raw materials, unloaded ALG/SOL and loaded ALG/SOL (left) and unloaded HYA/SOL and loaded HYA/SOL (right). Light orange lines stand for AZT peaks. (For interpretation of the references to colour in this figure legend, the reader is referred to the web version of this article.)

3.7. Scanning electron microscopy (SEM)

The AZT-loaded buccal films were also analysed by SEM, and the observations were consistent with the PXRD results. Specifically, HYA/SOL and ALG/SOL films showed the clear presence of flat (Fig. 4 B-C), rectangular crystals on the surface like those observed in the SEM image of pure crystalline AZT (Fig. 4 A).

In contrast, the CS-containing films displayed markedly different surface morphology (Fig. 4 D-F). No visible crystalline structures attributable to original AZT were observed, in line with the PXRD findings. These results further support the hypothesis of a solid-state interaction between AZT and the components of CS-based films, potentially leading to the formation of a new phase in which the drug is no longer detectable as free crystals.

Cross-sectional SEM imaging was performed to visualize the internal structure of the bilayer films and to distinguish the ethylcellulose

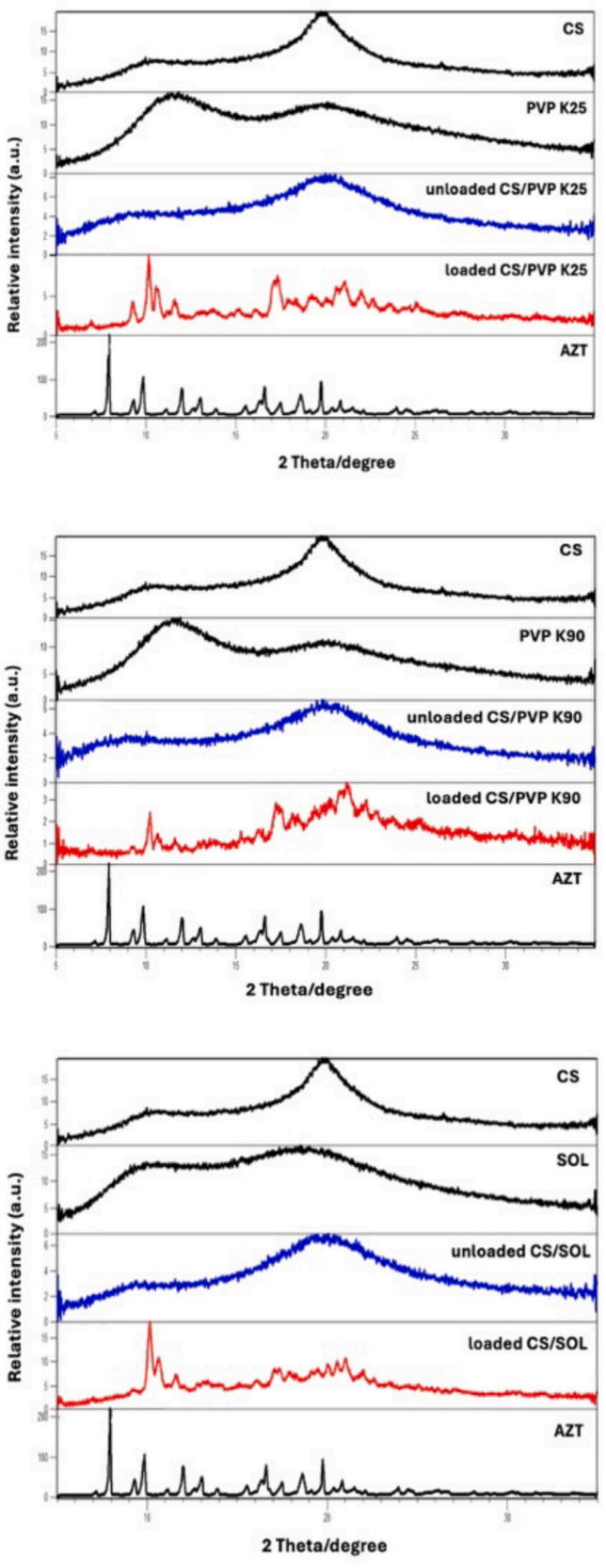

Fig. 3. PXRD of raw materials, unloaded CS/PVP K25 and loaded CS/PVP K25 (top), unloaded CS/PVP K90 and loaded CS/PVP K90 (center) and unloaded CS/SOL and loaded CS/SOL (bottom).

coating layer from the underlying drug-loaded matrix. Fig. 4G presents the HYA/SOL film as a representative example. The upper portion of the image clearly reveals a compact, continuous layer corresponding to the ethylcellulose coating, distinguishable by its uniform and dense appearance compared to the more porous and heterogeneous structure of the underlying film matrix. This morphological contrast confirms the deposition of the coating layer and highlights the bilayer architecture of the system.

3.8. FT-IR ATR

Fig. 5 shows FT-IR spectra acquired using the ATR technique. The red trace corresponds to the sample obtained from the interaction between AZT and lactic acid, prepared via dissolution followed by drying (see Section 2.10 for details). This spectrum is compared with those of pure AZT (black, top) and pure lactic acid (black, bottom).

In the red spectrum, a marked alteration of the spectral profile is observed compared to pure AZT:

- the characteristic bands of AZT (such as those between 1700–1600 cm^{-1}, corresponding to C=O and N–H groups (Islam et al., 2017) appear attenuated, shifted, or modified, suggesting loss of the original crystalline structure and formation of new molecular interactions.
- the most evident changes occur in the 1700 to 1500 cm^{-1} region (Islam et al., 2017) where the signals are broadened and less defined, indicating hydrogen bonding between functional groups of AZT and lactic acid.
- the absence of sharp bands typical of crystalline AZT supports the transition to an amorphous state or the formation of a new amorphous solid.
- when compared to lactic acid (black trace at the bottom), the red spectrum shares some common bands, but with clear shifts and modifications, which confirm the occurrence of interactions between the two components rather than a simple physical mixture.

These spectroscopic findings support the hypothesis of a strong interaction between AZT and lactic acid, likely involving the amino groups of the drug, which may have led to the formation of a new multicomponent solid.

3.9. Water uptake ability

Film hydration was investigated to predict their behaviour upon contact with biological fluids in the buccal cavity. Particularly, after film application on the buccal mucosa, the fluids wetting the mucosa can hydrate the formulations, providing the formation of systems with different viscosities. As a consequence, the water uptake behaviour influences the capacity of the films to adhere to the mucosa and the drug release and permeation (Timur et al., 2019).

Fig. 6 reports the water uptake profiles of the loaded films (primary layers). As can be seen, WU ability mainly depended on the polymeric composition of the film. Specifically, films composed of CS were characterised by a lower hydration ability with respect to ALG/SOL and HYA/SOL films ($p < 0.05$). This behaviour can be related to the ionization of the polymers. As a matter of fact, at pH 6.8, CS (pKa = 6.3) was slightly positively charged, thus determining the entry of a low amount of water. On the other hand, the carboxylic groups of ALG (pKa = 3.5) and HYA (pKa = 2.9) were completely negatively charged, thus providing an increased water uptake ability.

Moreover, a different trend was observed between all the samples. Particularly, water uptake profiles of CS-based films were biphasic with a fast initial phase (within 60–120 min) followed by a plateau phase. On the other hand, in the case of ALG/SOL and HYA/SOL a gradual hydration was observed. These findings can be ascribed to the formation of gels with different viscosity. In fact, in the case of ALG/SOL and HYA/

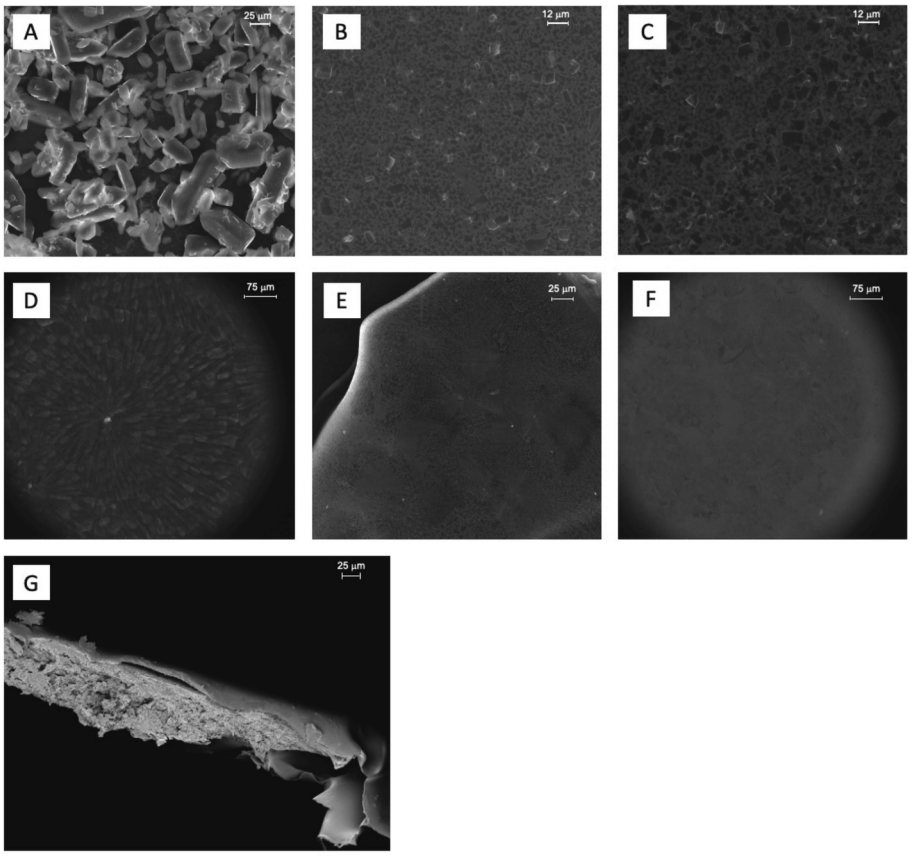

Fig. 4. SEM images of AZT at 400x (A), HYA/SOL at 700x (B), ALG/SOL at 800x (C), CS/PVP K25 at 200x (D), CS/PVP K90 at 400x (E), CS/SOL at 200x (F) and cross-sectional SEM image of the HYA/SOL bilayer buccal film.

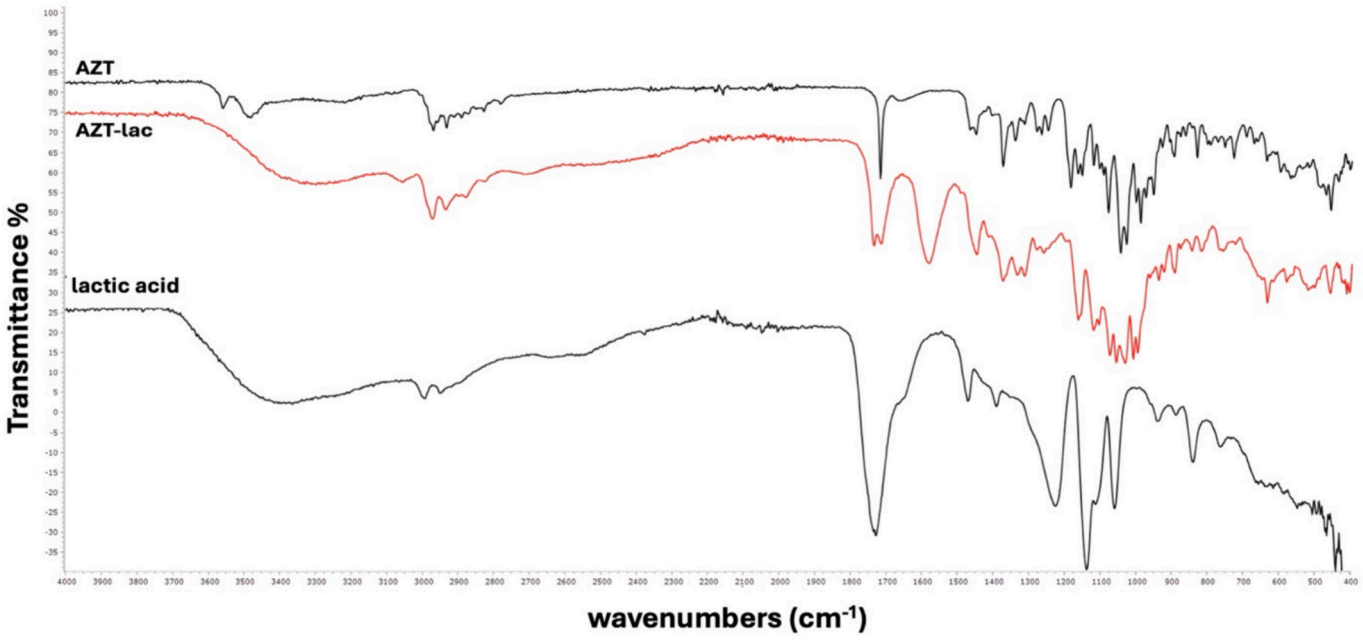

Fig. 5. FT-IR spectra of pure AZT (black, top), pure lactic acid (black, bottom), and the AZT-lac sample prepared by dissolution and drying (red, centre). (For interpretation of the references to colour in this figure legend, the reader is referred to the web version of this article.)

SOL, the hydration of films led to the formation of a highly viscous layer that represented a diffusion barrier for the water influx, while for CS-based films the lower viscosity determined the reaching of the maximum in a short time. However, despite the different viscosity of the starting CS solutions, no significant difference was observed between water uptake profiles of CS/PVP K25, CS/PVP K90 and CS/SOL ($p > 0.05$).

The presence of ethylcellulose backing layer did not impact on

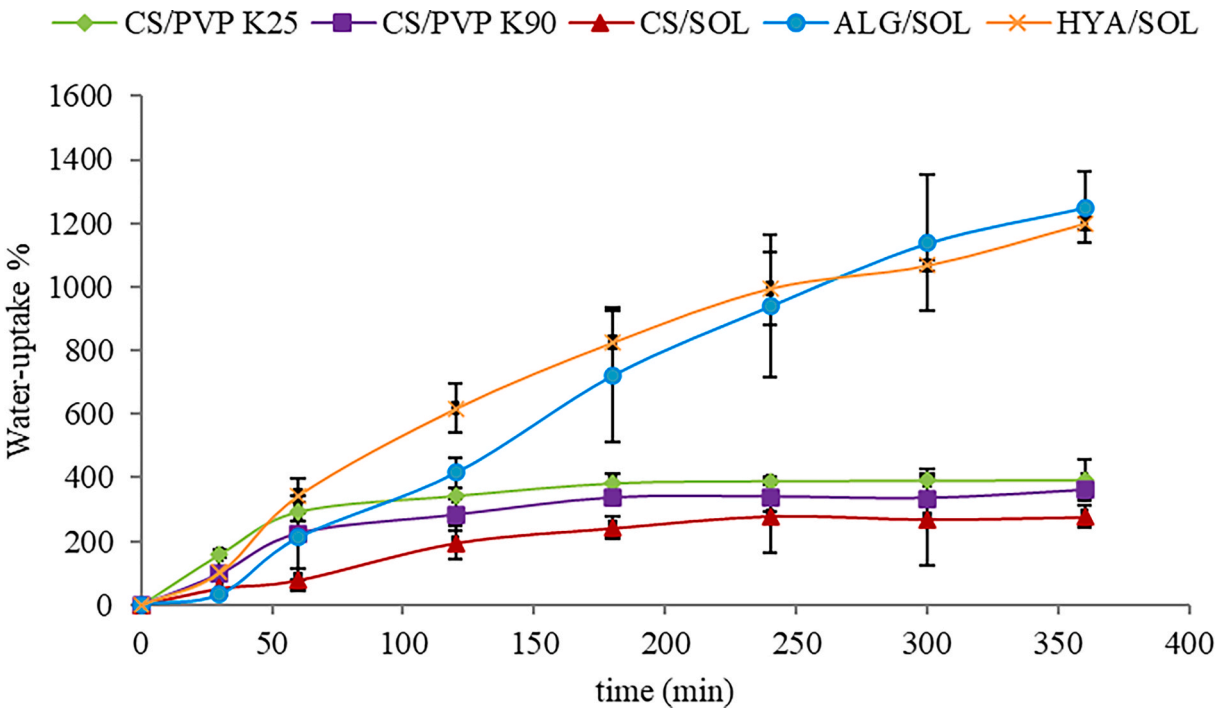

Fig. 6. Water uptake profiles obtained from primary polymeric layers containing AZT.

hydration properties (no difference was measured with respect to the primary layer, $p > 0.05$; data not shown).

3.10. *In vitro mucoadhesion ability and residence time*

Film ability to adhere to a mucosal surface is a crucial point for the buccal drug administration. As a matter of fact, a good mucoadhesion ability implies a long residence time in the buccal cavity, which in turn can result in high drug absorption. Mucoadhesion ability generally depends on different factors, such as polymer ionization and interaction with the mucus as well as hydration and interdiffusion of polymeric chains into the mucin (Boddupalli et al., 2010). To investigate the film ability to adhere to the mucosal surface, in this study two tests were carried out.

The first one allowed to determine the mucoadhesion ability by measuring the force needed to pull out the mucosa from primary polymeric layers. The greater the measured force, the stronger the contact between the mucosa and the formulation. The selected formulations presented similar values of detachment force. Specifically, for CS/PVP K25, CS/PVP K90 and CS/SOL the detachment forces were equal to 31 $\pm$ 2 dyne, 31 $\pm$ 4 dyne and 32 $\pm$ 3 dyne, respectively; while for ALG/SOL and HYA/SOL values of 30 $\pm$ 2 dyne and 27 $\pm$ 4 dyne, respectively, were registered. This result can be related to the presence of different hydrophilic groups of the primary polymeric films that can establish hydrogen bonds with the mucin chains (Giordani et al., 2020). Moreover, in the case of CS-based films, the polymer can also ionically interact with the negative charges of sialic and sulphonic acids of mucin (Russo et al., 2016). Additionally, the hydration and the consequent viscosity of the gelled film can have an impact on mucoadhesion ability.

In the second test, named *in vitro* residence time, the time needed to completely remove the film from the mucosal surface was measured. This test was conducted by using primary layers and bilayered films to evaluate the effect of the backing on the residence time. Primary layers composed of CS showed a short residence time and a complete detachment was observed within 10 min (no significant difference was observed between CS/PVP K25, CS/PVP K90 and CS/SOL, $p > 0.05$). This result was related to their rapid hydration, which determined an increase in weight leading to quick film detachment from the tissue. On the other hand, ALG/SOL and HYA/SOL, characterised by a slow hydration rate, were retained for a longer period of time (around 120 min; no significant difference was observed between ALG and HYA based films, $p > 0.05$); after this time the gelled films started to be removed from the tissue.

Moreover, the presence of the backing layer retarded the film detachment from the mucosa. Particularly, bilayered films based on CS remained attached to the mucosa until 60 min, while in the case of HYA and ALG the residence time was around 180 min. The latter results demonstrated that the ethylcellulose layer can protect the primary loaded layer films from the washing effect exerted from saliva and contribute enhancing the contact with the mucosa, determining an improvement in residence time.

3.11. *In vitro release studies*

The evaluation of drug release is extremely important considering that the release behaviour impacts on drug permeation and consequently on its bioavailability (Kumria et al., 2018). Drug release from buccal film depends on several factors, such as film hydration, drug solubility, and viscosity of the gelled system. Fig. 7 reports the drug release profiles obtained from the different primary polymeric layers and the Ctrl. As can be seen, Ctrl determined the immediate availability of the drug in the medium. On the contrary, a slower drug release was observed from the primary layers ($p < 0.05$). In fact, in this latter case, AZT must diffuse throughout the polymeric film before being released. Moreover, a different trend was observed for the developed formulations. Particularly, ALG/SOL and HYA/SOL determined the release of a lower amount of drug over the time with respect to CS-based films ($p < 0.05$). This behaviour was connected to the viscosity of the gelled films, which was strictly linked to that of the starting polymeric solutions (see section 3.2). Specifically, after hydration ALG and HYA based films provided the formation of gels with a greater viscosity with respect to the CS films. Consequently, the diffusion of the drug from a more viscous gel was slowed down. However, despite the different viscosity, no difference was observed between ALG and HYA based films, as well as between CS/PVP K25 and CS/PVP K90 ($p > 0.05$). Conversely, CS/SOL provided the release of a lower amount of AZT with respect to CS/PVP

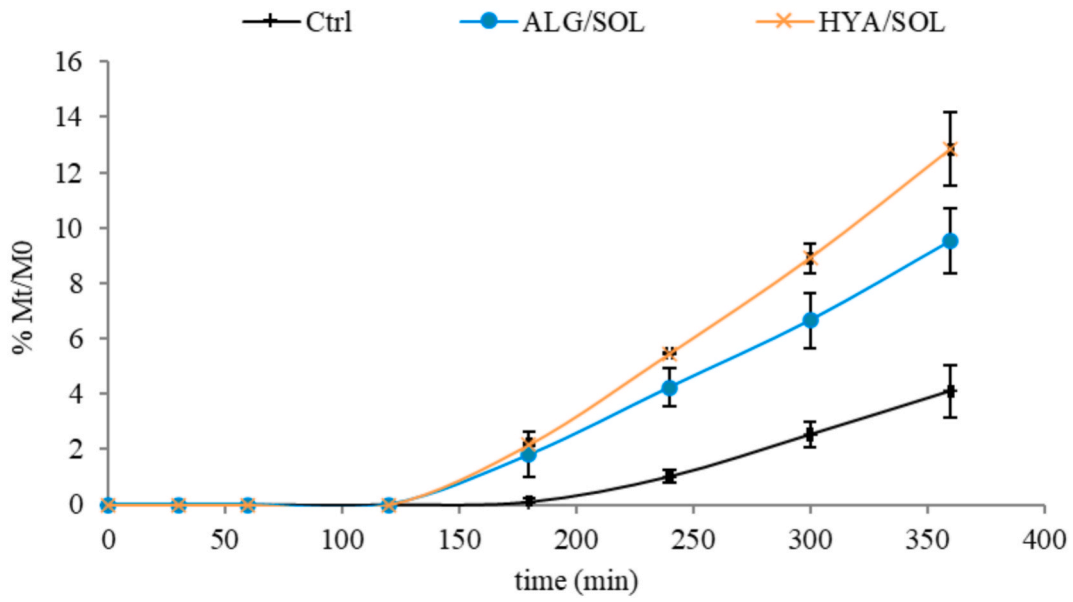

Fig. 7. *In vitro* release profiles from primary polymeric layers, Ctrl and AZT-lac.

films ($p < 0.05$). The lower release of AZT from CS/SOL films compared to CS/PVPs films may be attributed to the presence of SOL micelles, which can retain the drug and thereby reduce its diffusion rate (Fang et al., 2013; Shin et al., 2024).

Besides the viscosity, another factor influencing the drug release is connected to its solubility. In case of CS-based films an interaction between the drug and the lactic acid (previously highlighted via PXRD and finally explained through FT-IR characterization) occurred. This interaction could promote drug dissolution and consequently its release from CS based films. To confirm this result, another test was conducted by placing the powder obtained as described in section 2.10 (AZT-lact in the Fig. 7) in the release medium. Results obtained from this experiment confirmed the faster dissolution of AZT-lac with respect to the Ctrl (AZT powder).

In addition, the influence of the backing layer on drug release behaviour was investigated. Interestingly, bilayered films allowed the release of a lower amount of drug with respect to the primary polymeric layer. Particularly, no significant difference was observed between all the bilayered films ($p > 0.05$) and the mean percentage of drug, which was released from these samples was 11 ± 2 %, thus demonstrating that the method used for the application of the ethylcellulose layer can effectively decrease the drug release inside the buccal cavity. This latter finding is extremely important considering the need for limiting the bitter taste of AZT and minimizing the extent to which the drug is swallowed. As the release characteristics of CS/PVP were comparable, CS/PVP K90 was selected for further permeation studies.

3.12. Mechanical properties

The mechanical attributes of the films significantly impact their usability, patient compliance, and therapeutic effectiveness, while also ensuring reliable adhesion to the mucosa (Kis et al., 2019). Mechanical profiles of the different AZT-loaded films were evaluated with a texture analyzer. Burst strength (N), referring to the capacity of the film to resist rupture when subjected to pressure, was studied from the force-distance plot while the maximum applied pressure was calculated according to the area on which the compression force was applied. Results are reported in Table 3 for each formulation. CS/SOL based films presented the highest film burst strength (13.71 ± 3.78 N) which means they are the most stiff and hard to break, while HYA/SOL based films the lowest one (4.15 ± 0.29 N). Considering the maximum applied pressure, which can be related to the stress loaded onto the films, all of them presented a recorded value that is near to the one reported in literature for the oral mucosa (~ 1.54 MPa) (Choi et al., 2020). However, being less rigid and stiff, HYA/SOL (1.32 ± 0.09 MPa) and ALG/SOL (2.45 ± 0.32 MPa) were considered the most suitable ones for buccal application.

Table 3
Burst strength and maximum applied pressure on the different AZT-loaded buccal films.

Buccal Film	Burst strength (N)	Max. applied pressure (MPa)
CS/PVP K90	10.51 ± 2.26	3.35 ± 0.72
CS/SOL	13.71 ± 3.78	4.37 ± 1.20
ALG/SOL	7.70 ± 1.02	2.45 ± 0.32
HYA/SOL	4.15 ± 0.29	1.32 ± 0.09

3.13. In vitro permeation

Drug diffusion through the biological tissue and its accumulation can be considered predictive of the drug amount that can be absorbed and consequently reach the systemic circulation (Nair et al., 2009). However, drug diffusion and retention depend on several factors, like the physico- chemical properties of the drug, especially its solubility and repartition coefficient, its release from the formulation and the characteristics of the tissue. As mentioned above, in this study we selected the oesophageal mucosa as a model of human buccal tissue, since it has been reported that these membranes were comparable in terms of composition, structure and permeability ability (Diaz del Consuelo et al., 2005). Fig. 8 reports the cumulative percentage amount of AZT permeated from bilayered films (HYA/SOL and ALG/SOL) and Ctrl through the oesophageal epithelium. As can be seen, AZT permeated the membrane reaching after 360 min a cumulative percentage amount equal to 4.09 ± 0.94 %. On the other hand, despite the lower drug release, ALG/SOL and HYA/SOL provided an increase in drug permeation with respect to the Ctrl ($p < 0.05$). This result can be ascribed to the presence of SOL micelles, which can favour the drug diffusion through the membrane, in agreement with previous findings (Piazzini et al., 2020; Sipos et al., 2023). On the other hand, in the case of CS-based films (CS/PVP K90 and CS/SOL) no drug permeation was observed (concentrations of the receptor chamber under the limit of detection). This latter observation was related to the presence of the new form of the drug in these films. To

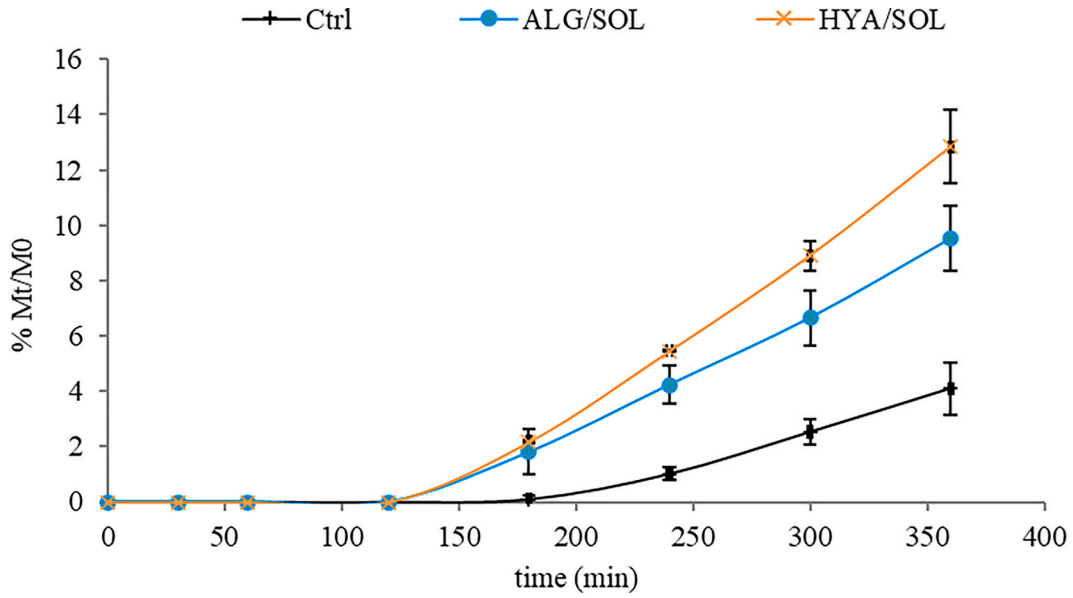

Fig. 8. *In vitro* permeation profiles from Ctrl, ALG/SOL and HYA/SOL bilayered films.

confirm this result, the powder obtained as described in section 2.10 (AZT-lac) was placed in the donor chamber and tested for its ability to diffuse through the membrane. Results obtained from this experiment confirmed that the new hydrophilic form of AZT, possessing high solubilization capacity (as described in section 3.11) was not able to diffuse through the lipophilic environment of the tissue.

Permeation studies were also conducted using the primary monolayer film to evaluate the influence of the backing on drug permeation. As a matter of fact, the presence of a backing layer may provide an occlusive effect and consequently increase hydration of the tissue, thus finally improving drug permeation. Nevertheless, in this study no significant difference was observed between mono and bilayered films ($p > 0.05$, data not shown). This finding agreed with previous findings, demonstrating that the backing layer did not increase the hydration of oesophageal epithelium, which – being a nonkeratinized tissue – is basically characterised by high water content (Diaz del Consuelo et al., 2005).

Furthermore, flux values were equal to 14.90 ± 2.33 μg/cm^2*min, 19.32 ± 3.75 μg/cm^2*min and 23.34 ± 0.86 μg/cm^2*min for Ctrl, ALG/SOL and HYA/SOL, respectively. Considering the permeation flux values, the required area of the selected films was calculated by using the following equation:

$$C_{ss} = J^*A/Cl$$

where C_{ss} is the concentration at the steady state, Cl is the clearance and J is the flux. The pharmacokinetic data in children reported a C_{ss} of 0.07 μg/mL and Cl of 1.23 L/h/kg (Nahata et al., 1993; Schmoldt et al., 1975). Based on these data, the film surface area required to achieve effective plasma concentration for children of 20 kg (estimated age 6 years) (Carasco et al., 2016; Souares et al., 2010) were 1.49 cm^2 and 1.23 cm^2 for ALG/SOL and HYA/SOL, respectively. These surface areas are compatible with buccal application in paediatric population.

ALG/SOL and HYA/SOL were further selected to evaluate the amount of AZT able to be retained in the oesophageal epithelium and compared to the Ctrl. The measurement of the drug amount retained inside the tissue represents an important point since it can be assumed that this fraction is available to pass into the systemic circulation, thus contributing to the final therapeutic effect. Data obtained from this study demonstrated that the presence of the films allowed to increase the retention of the drug inside the oesophageal epithelium with respect to the Ctrl ($p < 0.05$). In fact, the cumulative percentage amounts in the tissue measured after 360 min of permeation were equal to 9.71 ± 1.68 % and 9.97 ± 3.04 % for ALG/SOL and HYA/SOL, respectively; while only 3.04 ± 0.63 % was retained in the presence of the Ctrl. This result could be attributed to the presence of SOL micelles which can determine the accumulation of AZT inside the tissue, in agreement with previous observations (Varela-Garcia et al., 2018).

To sum up, these results confirmed the potential of the developed formulations, particularly of ALG/SOL and HYA/SOL, to provide effective permeation and retention of AZT through/inside the biological tissue, as well as their potential to be easily applied in the buccal cavity of children.

3.14. Antimicrobial properties

To assess the antimicrobial activity of AZT-loaded films, *Staphylococcus aureus* ATCC 29213 and *Escherichia coli* ATCC 11105 were chosen as representative Gram-positive and Gram-negative test bacteria, respectively. CS/SOL was selected among the CS based films in order to evaluate the antimicrobial properties of the new form of AZT. HYA/SOL film was also chosen considering its ability to promote drug permeation. MIC values were determined by microdilution assay after 24 h of incubation. Free AZT confirmed MIC values of 1 μg/mL on both microbial strains, in accordance with previously reported data (Abruzzo et al., 2022; Lugli et al., 2025). AZT released by CS/SOL and HYA/SOL films retained the antimicrobial activity, as demonstrated by the invariant MIC values (1 μg/mL for both samples). Moreover, unloaded films did not interfere with microbial growth. These findings demonstrated that the preparation process did not impact the antimicrobial properties of AZT. Furthermore, AZT antimicrobial properties were maintained in the case of CS based films when a new form of the drug was formed, as well as in HYA/SOL film.

4. Conclusion

Within this study, for the first time, a screening involving different mucoadhesive polymers in association with several solubilizing agents was conducted with the final aim of obtaining bilayered buccal films for AZT administration in children. Results allowed selecting adequate materials to obtain a primary polymeric layer, able to adhere to the buccal mucosa and control drug release over time, and a secondary backing layer, which could limit drug diffusion in the buccal cavity. Specifically, the employment of CS in association with PVPs or SOL

provided the formation of films composed of a new form of the drug, which occurred with the interaction between AZT and lactic acid. Although permeation studies highlighted that no drug diffusion through the tissue occurred with CS-based films, the identification of a new form of AZT with improved solubility capacity and unaltered antimicrobial activity opens promising scenarios in the field of local delivery systems for AZT administration. Alongside, our study allowed to identify ALG/SOL and HYA/SOL as useful bilayered films for buccal AZT administration in children. As a matter of fact, these films presented interesting properties in terms of manufacturing method and functional properties. Specifically, they were easily developed through the solvent casting method and removed from the mould. Moreover, they were characterised by a good homogeneity in terms of weight, thickness and drug content and presented good mucoadhesion and ability to control the drug release. Furthermore, the presence of the backing layer could assure the unidirectional drug absorption towards the mucosa and limit the drug release in the buccal cavity, thus potentially permitting the reduction of the bitter taste perception. Finally, HYA/SOL film favoured the drug permeation through the buccal mucosa, maintaining at the same time the antimicrobial activity of the drug. Overall, HYA/SOL has great potential as a buccal drug delivery system for the systemic absorption of AZT due to its expected ease of use, increased patient compliance and improved drug permeation.

CRediT authorship contribution statement

Giulia Bondi: Writing – original draft, Methodology, Investigation, Formal analysis, Data curation. **Ilenia D'Abbrunzo:** Writing – original draft, Methodology, Investigation, Formal analysis, Data curation, Conceptualization. **Dritan Hasa:** Writing – review & editing, Supervision, Investigation, Data curation, Conceptualization. **Carola Parolin:** Writing – original draft, Methodology, Investigation. **Beatrice Vitali:** Writing – review & editing. **Serena Bertoni:** Writing – original draft. **Anna Imbriano:** Writing – original draft. **Cinzia Pagano:** Writing – review & editing. **Costanza Fratini:** Writing – original draft, Methodology, Investigation, Data curation. **Beatrice Sabbatini:** Methodology, Investigation, Formal analysis, Data curation. **Federica Bigucci:** Writing – review & editing, Supervision, Data curation, Conceptualization. **Angela Abruzzo:** Writing – review & editing, Writing – original draft, Supervision, Resources, Project administration, Funding acquisition, Formal analysis, Data curation, Conceptualization.

Declaration of competing interest

The authors declare the following financial interests/personal relationships which may be considered as potential competing interests: Angela Abruzzo reports financial support was provided by Ministero dell'Università e della Ricerca with the project "3D-printed antibiotic oral dosage forms for paediatric use" [p3Diatrics] which has been granted with Project of Relevant National Interest (PRIN 2022); Project ID: 2022FRNFMT. If there are other authors, they declare that they have no known competing financial interests or personal relationships that could have appeared to influence the work reported in this paper.

Acknowledgements

The study was funded by Ministero dell'Università e della Ricerca with the project "3D-printed antibiotic oral dosage forms for paediatric use" [p3Diatrics] which has been granted with Project of Relevant National Interest (PRIN 2022); Project ID: 2022FRNFMT.

Data availability

Data will be made available on request.

References

Abdella, S., Afinjuomo, F., Song, Y., Upton, R., Garg, S., 2022. Mucoadhesive Buccal Film of Estradiol for Hormonal Replacement Therapy: Development and In-Vivo Performance Prediction. Pharmaceutics 14, 542. https://doi.org/10.3390/pharmaceutics14030542.

Abruzzo, A., Nicoletta, F.P., Dalena, F., Cerchiara, T., Luppi, B., Bigucci, F., 2017. Bilayered buccal films as child-appropriate dosage form for systemic administration of propranolol. Int. J. Pharm. 531, 257–265. https://doi.org/10.1016/j.ijpharm.2017.08.070.

Abruzzo, A., Parolin, C., Rossi, M., Vitali, B., Cappadone, C., Bigucci, F., 2022. Development and Characterization of Azithromycin-Loaded Microemulsions: a Promising Tool for the Treatment of Bacterial Skin Infections. Antibiotics 11, 1040. https://doi.org/10.3390/antibiotics11081040.

Al-Dhubiab, B.E., Nair, A.B., Kumria, R., Attimarad, M., Harsha, S., 2016. Development and evaluation of buccal films impregnated with selegiline-loaded nanospheres. Drug Deliv. 23, 2154–2162. https://doi.org/10.3109/10717544.2014.948644.

Aucamp, M., Odendaal, R., Liebenberg, W., Hamman, J., 2015. Amorphous azithromycin with improved aqueous solubility and intestinal membrane permeability. Drug Dev. Ind. Pharm. 41, 1100–1108. https://doi.org/10.3109/03639045.2014.931967.

Bagan, J., Paderni, C., Termine, N., Campisi, G., Lo Russo, L., Compilato, D., Di Fede, O., 2012. Mucoadhesive Polymers for Oral Transmucosal Drug delivery: a Review. CPD 18, 5497–5514. https://doi.org/10.2174/138161212803307545.

Boddupalli, B., Mohammed, ZulkarN.K., Nath, R., Banji, D., 2010. Mucoadhesive drug delivery system: An overview. J Adv Pharm Technol Res 1, 381. doi: 10.4103/0110-5558.76436.

Boza, I.A.F., da Silva, S.L., Guedes, N.B., Bazzo, G.C., Stulzer, H.K., 2025. Pediatric Formulation Optimization using a Rational Design: Exploring Amorphous Solid Dispersion Technology with Terbinafine Hydrochloride as a Case Study. AAPS PharmSciTech. 26, 40. https://doi.org/10.1208/s12249-024-03012-4.

Carasco, C.F., Fletcher, P., Maconochie, I., 2016. Review of commonly used age-based weight estimates for paediatric drug dosing in relation to the pharmacokinetic properties of resuscitation drugs. Brit. J. Clin. Pharma 81, 849–856. https://doi.org/10.1111/bcp.12876.

Choi, J.J.E., Zwirner, J., Ramani, R.S., Ma, S., Hussaini, H.M., Waddell, J.N., Hammer, N., 2020. Mechanical properties of human oral mucosa tissues are site dependent: a combined biomechanical, histological and ultrastructural approach. Clinical Exp. Dental Res. 6, 602–611. https://doi.org/10.1002/cre2.305.

Cockerill, 2012. Methods for dilution antimicrobial susceptibility tests for bacteria that grow aerobically: approved standard, ninth edition. Clinical and Laboratory Standards Institute.

Cornilă, A., Iurian, S., Tomuță, I., Porfire, A., 2022. Orally dispersible dosage forms for paediatric use: current knowledge and development of nanostructure-based formulations. Pharmaceutics 14, 1621. https://doi.org/10.3390/pharmaceutics14081621.

Corzo-Martínez, M., Mohan, M., Dunlap, J., Harte, F., 2015. Effect of Ultra-High pressure Homogenization on the Interaction between Bovine Casein Micelles and Ritonavir. Pharm. Res. 32, 1055–1071. https://doi.org/10.1007/s11095-014-1518-9.

Diaz del Consuelo, I., Pizzolato, G.-P., Falson, F., Guy, R.H., Jacques, Y., 2005. Evaluation of pig esophageal mucosa as a permeability barrier model for buccal tissue. J. Pharm. Sci. 94, 2777–2788. https://doi.org/10.1002/jps.20409.

Domingues, C., Jarak, I., Veiga, F., Dourado, M., Figueiras, A., 2023. Pediatric Drug Development: reviewing challenges and Opportunities by Tracking innovative Therapies. Pharmaceutics 15, 2431. https://doi.org/10.3390/pharmaceutics15102431.

Dung, P.-T.-P., Trinh, T.-D., Nguyen, Q.-H., Nguyen, H.-M., Nguyen, N.-C., Tran, N.-B., Tran, C.-S., Nguyen, T.-H.-N., Tung, N.-T., 2023. Development of taste-masking microcapsules containing azithromycin by fluid bed coating for powder for suspension and *in vivo* evaluation. J. Microencapsul. 40, 345–356. https://doi.org/10.1080/02652048.2023.2209639.

Fang, X., Chen, Sha, X., Jiang, Chen, Y., Ren, 2013. Pluronic P105/F127 mixed micelles for the delivery of docetaxel against Taxol-resistant non-small cell lung cancer: optimization and in vitro, in vivo evaluation. IJN 73. doi: 10.2147/IJN.S38221.

Fiese, E.F., Steffen, S.H., 1990. Comparison of the acid stability of azithromycin and erythromycin a. J. Antimicrob. Chemother. 25, 39–47. https://doi.org/10.1093/jac/25.suppl_A.39.

Gilhotra, R., Nagpal, K., Mishra, D., 2011. Azithromycin novel drug delivery system for ocular application. Int J Pharma Investig 1, 22. https://doi.org/10.4103/2230-973X.76725.

Giordani, B., Abruzzo, A., Prata, C., Nicoletta, F.P., Dalena, F., Cerchiara, T., Luppi, B., Bigucci, F., 2020. Ondansetron buccal administration for paediatric use: a comparison between films and wafers. Int. J. Pharm. 580, 119228. https://doi.org/10.1016/j.ijpharm.2020.119228.

Gittings, S., Turnbull, N., Henry, B., Roberts, C.J., Gershkovich, P., 2015. Characterisation of human saliva as a platform for oral dissolution medium development. Eur. J. Pharm. Biopharm. 91, 16–24. https://doi.org/10.1016/j.ejpb.2015.01.007.

Guideline on Validation of Analytical Procedures, 2022.

Guimarães, M., Somville, P., Vertzoni, M., Fotaki, N., 2021. Investigating the critical Variables of Azithromycin Oral Absorption using In Vitro Tests and PBPK Modeling. J. Pharm. Sci. 110, 3874–3888. https://doi.org/10.1016/j.xphs.2021.09.013.

Islam, M.R., Moghal, M.M.R., Bari, F.S.N.U., Mamun, E.A., 2017. Design and Development of Bi-layered Sustained Release Azithromycin Tablets. Dhaka Univ. J. Pharm. Sci 15, 227–234. https://doi.org/10.3329/dujps.v15i2.30942.

Jiang, S., Mou, Y., He, H., Yang, D., Qin, L., Zhang, F., Zhang, P., 2019. Preparation and evaluation of self-assembly Soluplus® -sodium cholate-phospholipid ternary mixed

micelles of docetaxel. Drug Dev. Ind. Pharm. 45, 1788–1798. https://doi.org/10.1080/03639045.2019.1660365.
Kauss, T., Gaubert, A., Boyer, C., Ba, B.B., Manse, M., Massip, S., Léger, J.-M., Fawaz, F., Lembege, M., Boiron, J.-M., Lafarge, X., Lindegardh, N., White, N.J., Olliaro, P., Millet, P., Gaudin, K., 2013. Pharmaceutical development and optimization of azithromycin suppository for paediatric use. Int. J. Pharm. 441, 218–226. https://doi.org/10.1016/j.ijpharm.2012.11.040.
Kis, N., Kovács, A., Budai-Szűcs, M., Gácsi, A., Csányi, E., Csóka, I., Berkó, S., 2019. Investigation of Silicone-Containing Semisolid in Situ Film-Forming Systems using QbD Tools. Pharmaceutics 11, 660. https://doi.org/10.3390/pharmaceutics11120660.
Korelc, K., Larsen, B.S., Gašperlin, M., Tho, I., 2023. Water-soluble chitosan eases development of mucoadhesive buccal films and wafers for children. Int. J. Pharm. 631, 122544. https://doi.org/10.1016/j.ijpharm.2022.122544.
Kumria, R., Al-Dhubiab, B.E., Shah, J., Nair, A.B., 2018. Formulation and evaluation of Chitosan-based Buccal Bioadhesive Films of Zolmitriptan. J. Pharm. Innov. 13, 133–143. https://doi.org/10.1007/s12247-018-9312-6.
Kurakula, M., Rao, G.S.N.K., 2020. Pharmaceutical assessment of polyvinylpyrrolidone (PVP): As excipient from conventional to controlled delivery systems with a spotlight on COVID-19 inhibition. J. Drug Delivery Sci. Technol. 60, 102046. https://doi.org/10.1016/j.jddst.2020.102046.
Lam, J.K.W., Xu, Y., Worsley, A., Wong, I.C.K., 2014. Oral transmucosal drug delivery for pediatric use. Adv. Drug Deliv. Rev. 73, 50–62. https://doi.org/10.1016/j.addr.2013.08.011.
Latif, S., Vandana, K., Thimmashetty, J., Dalvi, P., 2016. Azithromycin buccal patch in treatment of chronic periodontitis. Indian J Pharmacol 48, 208. https://doi.org/10.4103/0253-7613.178829.
Lo, J.B., Appel, L.E., Herbig, S.M., McCray, S.B., Thombre, A.G., 2009. Formulation design and pharmaceutical development of a novel controlled release form of azithromycin for single-dose therapy. Drug Dev. Ind. Pharm. 35, 1522–1529. https://doi.org/10.3109/03639040903037223.
Lugli, S., Abruzzo, A., Parolin, C., Vitali, B., Bolognesi, M.L., Brucale, M., Valle, F., Cerchiara, T., Luppi, B., Bigucci, F., 2025. Mucoadhesive polymer-coated liposomes as a promising approach to counteract bacteria responsible for aerobic vaginitis. Int. J. Pharm. 677, 125667. https://doi.org/10.1016/j.ijpharm.2025.125667.
Luke, D.R., Foulds, G., 1997. Disposition of oral azithromycin in humans*. Clin. Pharmacol. Ther. 61, 641–648. https://doi.org/10.1016/S0009-9236(97)90098-9.
Marques, M.R.C., Loebenberg, R., Almukainzi, M., 2011. Simulated Biological Fluids with possible Application in Dissolution Testing. Dissolution Technol. 18, 15–28. https://doi.org/10.14227/DT180311P15.
Mashaqbeh, H., Obaidat, R.M., Alsmadi, M.M., 2024. Solvent-free method for masking the bitter taste of azithromycin dihydrate using supercritical fluid technology. Drug Dev. Ind. Pharm. 50, 102–111. https://doi.org/10.1080/03639045.2023.2298892.
Muzib, Y.i., Kumari, K.s., 2011. Mucoadhesive buccal films of glibenclamide: Development and evaluation. Int J Pharma Investig 1, 42. https://doi.org/10.4103/2230-973X.76728.
Nahata, M.C., Koranyi, K.I., Gadgil, S.D., Hilligoss, D.M., Fouda, H.G., Gardner, M.J., 1993. Pharmacokinetics of azithromycin in pediatric patients after oral administration of multiple doses of suspension. Antimicrob. Agents Chemother. 37, 314–316. https://doi.org/10.1128/AAC.37.2.314.
Nair, A., Reddy, C., Jacob, S., 2009. Delivery of a classical antihypertensive agent through the skin by chemical enhancers and iontophoresis. Skin Res. Technol. 15, 187–194. https://doi.org/10.1111/j.1600-0846.2009.00350.x.
Nair, A.B., Kumria, R., Harsha, S., Attimarad, M., Al-Dhubiab, B.E., Alhaider, I.A., 2013. In vitro techniques to evaluate buccal films. J. Control. Release 166, 10–21. https://doi.org/10.1016/j.jconrel.2012.11.019.
Piazzini, V., Landucci, E., Urru, M., Chiarugi, A., Pellegrini-Giampietro, D.E., Bilia, A.R., Bergonzi, M.C., 2020. Enhanced dissolution, permeation and oral bioavailability of aripiprazole mixed micelles: In vitro and in vivo evaluation. Int. J. Pharm. 583, 119361. https://doi.org/10.1016/j.ijpharm.2020.119361.
Russo, E., Selmin, F., Baldassari, S., Gennari, C.G.M., Caviglioli, G., Cilurzo, F., Minghetti, P., Parodi, B., 2016. A focus on mucoadhesive polymers and their application in buccal dosage forms. J. Drug Delivery Sci. Technol. 32, 113–125. https://doi.org/10.1016/j.jddst.2015.06.016.
Schmoldt, A., Benthe, H.F., Haberland, G., 1975. Digitoxin metabolism by rat liver microsomes. Biochem. Pharmacol. 24, 1639–1641.
Shin, Y., Choi, J.-Y., Yoon, M., Yoo, M., Shin, D.H., Lee, J.-W., 2024. Evaluation of Anticancer Efficacy of D-α-Tocopheryl Polyethylene-Glycol Succinate and Soluplus® mixed Micelles Loaded with Olaparib and Rapamycin against Ovarian Cancer. IJN 19, 7871–7893. https://doi.org/10.2147/IJN.S468935.
Sipos, B., Bella, Z., Gróf, I., Veszelka, S., Deli, M.A., Szűcs, K.F., Sztojkov-Ivanov, A., Ducza, E., Gáspár, R., Kecskeméti, G., Janáky, T., Volk, B., Budai-Szűcs, M., Ambrus, R., Szabó-Révész, P., Csóka, I., Katona, G., 2023. Soluplus® promotes efficient transport of meloxicam to the central nervous system via nasal administration. Int. J. Pharm. 632, 122594. https://doi.org/10.1016/j.ijpharm.2023.122594.
Souares, A., Lalou, R., Senghor, P., Le Hesran, J.Y., 2010. Child age or weight: difficulties related to the prescription of the right dosage of antimalarial combinations to treat children in Senegal. Trans. R. Soc. Trop. Med. Hyg. 104, 104–109. https://doi.org/10.1016/j.trstmh.2009.07.018.
Swainston Harrison, T., Keam, S.J., 2007. Azithromycin Extended Release: a Review of its use in the Treatment of Acute Bacterial Sinusitis and Community-acquired Pneumonia in the US. Drugs 67, 773–792. https://doi.org/10.2165/00003495-200767050-00010.
Teodorescu, M., Bercea, M., 2015. Poly(vinylpyrrolidone) – a Versatile Polymer for Biomedical and beyond Medical applications. Polym.-Plast. Technol. Eng. 54, 923–943. https://doi.org/10.1080/03602559.2014.979506.
Timoumi, S., Mangin, D., Peczalski, R., Zagrouba, F., Andrieu, J., 2014. Stability and thermophysical properties of azithromycin dihydrate. Arab. J. Chem. 7, 189–195. https://doi.org/10.1016/j.arabjc.2010.10.024.
Timur, S.S., Yüksel, S., Akca, G., Şenel, S., 2019. Localized drug delivery with mono and bilayered mucoadhesive films and wafers for oral mucosal infections. Int. J. Pharm. 559, 102–112. https://doi.org/10.1016/j.ijpharm.2019.01.029.
Tung, N.-T., Tran, C.-S., Nguyen, T.-L., Hoang, T., Trinh, T.-D., Nguyen, T.-N., 2018. Formulation and biopharmaceutical evaluation of bitter taste masking microparticles containing azithromycin loaded in dispersible tablets. Eur. J. Pharm. Biopharm. 126, 187–200. https://doi.org/10.1016/j.ejpb.2017.03.017.
Varela-Garcia, A., Concheiro, A., Alvarez-Lorenzo, C., 2018. Soluplus micelles for acyclovir ocular delivery: Formulation and cornea and sclera permeability. Int. J. Pharm. 552, 39–47. https://doi.org/10.1016/j.ijpharm.2018.09.053.